

# Generalized Signal Phase Inversion-Based NOMA Technique for 6G Integrated Sensing and Communication Systems

Juyeong Baek, Young-Seok Lee, *Student Member, IEEE*, In-Ki Lee, and Bang Chul Jung, *Senior Member, IEEE*

**Abstract**—In this paper, we propose a novel uplink signal phase inversion-based non-orthogonal multiple access (SPIN-NOMA) technique to effectively suppress mutual interference in integrated sensing and communication (ISAC) systems. Specifically, we consider an ISAC system where a base station (BS) operates as a monostatic radar to sense targets while simultaneously receiving communication signals from multiple user equipments (UEs). We identify limitations in the conventional SPIN-NOMA approach and introduce technical advancements to support *high-order* modulation schemes and an *arbitrary* number of UEs. Additionally, we theoretically derive the generalized bit-error rate (BER) performance as a function of modulation order and the number of UEs, employing linear zero-forcing beamforming. Extensive simulations confirm that the proposed SPIN-NOMA technique significantly outperforms the conventional approach in terms of both sensing and communication performance. Furthermore, the simulation results align closely with the derived theoretical BER expressions, confirming their accuracy.

**Index Terms**—6G, integrated sensing and communication (ISAC), bit-error rate (BER), non-orthogonal multiple access (NOMA), monostatic radar.

## I. INTRODUCTION

Integrated sensing and communication (ISAC) systems have recently emerged as a promising paradigm for next-generation mobile networks, as they enable the convergence of heterogeneous services by jointly supporting communication and radar sensing through shared hardware and waveforms [1]. Recently, various studies have been conducted to effectively integrate communication and sensing functionalities [2], [3], [5]. In [2], a direct relationship between kinematic parameters—such as angle, delay, and Doppler—and the communication channel was established, and a probabilistic representation of the orthogonal time frequency space-based multiple-input multiple-output (OTFS-MIMO) system was derived. In [3], a cloud-edge-user three-tier architecture is proposed for an integrated sensing, communication, and computation system. In [5], a robust dual-functional waveform design framework was proposed to address channel uncertainties. The framework is formulated as a min-max optimization problem, where the minimization step derives the optimal waveform, while the maximization step accounts for the worst-case characteristics of the communication channel under uncertainty.

Effective interference mitigation and resource management techniques are essential to balance the trade-off between

sensing and communication functionalities [5], [6]. In [5], an optimization problem was formulated to mitigate interference resulting from overlapping coverage areas in multi-cell ISAC scenarios. Similarly, [6] proposed a method to reduce mutual interference by partially overlapping wireless resources allocated for sensing and communication functions, while also deriving the outage probability mathematically.

Non-orthogonal multiple access (NOMA) has garnered attention for its potential to simultaneously process communication and sensing signals in ISAC systems [7]–[12]. The studies in [8] and [9] proposed NOMA-based ISAC signal processing techniques that exploit successive interference cancellation (SIC) to mitigate mutual interference between communication and sensing signals. Building on this idea, [8] further analyzed how different SIC ordering strategies affect the performance of NOMA-ISAC, while [9] mathematically analyzed the outage probability for both communication and sensing. An uplink NOMA-ISAC short-packet transmission framework considering different SIC detection orders was introduced in [10]. In addition, the authors formulated a weighted sum-rate maximization problem and developed alternating optimization algorithms to address the non-convexity arising from rate loss due to short-packet transmission. However, error propagation in the SIC process remains a critical issue that negatively affects the overall communication performance. However, error propagation in SIC remains a critical issue. To address this limitation of SIC, [11] proposed the signal phase inversion-based NOMA (SPIN-NOMA) technique to mitigate mutual interference in uplink ISAC systems, where a single base station (BS) simultaneously receives communication signals from multiple user equipments (UEs) and performs target sensing via monostatic radar. This technology enables effective separation of communication signals by inverting the phase of the sensing signal and transmitting it across two time slots within the coherence time, allowing for a simple linear combination to achieve separation. Furthermore, [12] analyzed the bit-error rate (BER) performance of the SPIN-NOMA technique in a specific case where two quadrature phase-shift keying (QPSK) symbols are combined to form a 16-point constellation. However, it did not consider optimal constellation design or bit mapping strategies from a communication performance perspective, leaving room for further improvement. Since the communication signals are detected and subsequently canceled from the received signal via SIC, the accuracy of communication signal detection directly affects the estimation of the sensing channel. To the best of our knowledge, a generalized theoretical analysis of the SPIN-NOMA technique considering arbitrary square quadrature amplitude modulation (QAM) has yet to be conducted.

In this paper, we propose a novel SPIN-NOMA scheme that incorporates a communication constellation design to

This work was supported in part by the NRF through the Korean Government (MSIT) under Grant No. RS-2025-02303435 and in part by the Intelligent Technology Development Program on Disaster Response and Emergency Management (2022-MOIS37-005). *The corresponding authors are In-Ki Lee and Bang Chul Jung.*

J. Baek, Y. -S. Lee, and B. C. Jung are with the Department of Electrical and Computer Engineering, Ajou University, Suwon 16499, South Korea (e-mail: jybaek@ajou.ac.kr; youngseoklee@ajou.ac.kr; bcjung@ajou.ac.kr).

I. -K. Lee is with the Satellite Communication Infra Research Section, Electronics and Telecommunications Research Institute, Daejeon 34129, South Korea (email: popularity1@etri.re.kr).

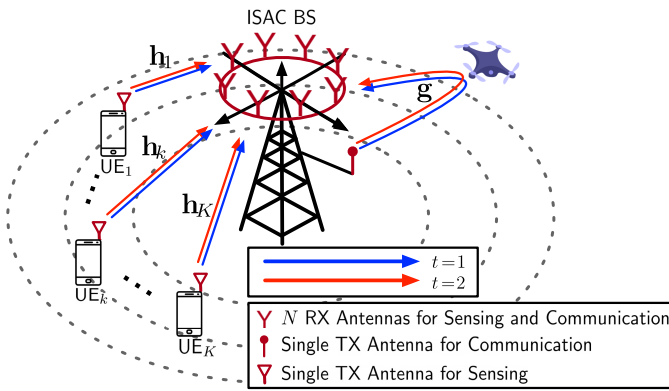


Fig. 1. System model of uplink SPIN-NOMA with a single BS, a single target, and  $K$  UEs.

enhance performance over conventional approaches. We consider arbitrary square QAM and conduct a theoretical analysis of the BER performance and diversity order under a linear zero-forcing (ZF) receiver. Simulation results show that the proposed constellation design outperforms existing schemes in terms of BER and normalized mean square error (NMSE) for sensing channel estimation, while maintaining the same data rate. Finally, we verify that the theoretical analysis closely matches the simulation results.

## II. SYSTEM MODEL

We consider an uplink ISAC-NOMA system where a single ISAC BS with a transmit antenna for sensing and an  $N$ -element uniform circular array (UCA) of receive antennas simultaneously senses a single passive target and supports  $K$  UEs, as depicted in Fig. 1. We assume that each single-antenna UE simultaneously transmits communication signals to the ISAC BS over two time slots within the channel coherence time, during which the wireless channel remains constant. Meanwhile, the ISAC BS transmits sensing signals for monostatic radar sensing of a nearby passive target over the same two time slots. We define  $\mathbf{h}_k \in \mathbb{C}^N$  as a communication channel vector from  $k \in \{1, \dots, K\}$ -th UE to the ISAC BS. We assume that the communication channels follow the independent and identically distributed Rayleigh fading channel model, i.e.,  $\mathbf{h}_k \sim \mathcal{CN}(\mathbf{0}, l_k^{-\alpha} \mathbf{I}_N)$ , where  $\mathbf{I}_N$ ,  $l_k$ , and  $\alpha$  denote the identity matrix of size  $N$ , a distance between the  $k$ -th UE and ISAC BS, and path-loss exponent, respectively. The sensing channel vector,  $\mathbf{g} \in \mathbb{C}^N$ , represents a bidirectional radar channel as

$$\mathbf{g} = \zeta e^{-j2\pi(f_c + \Delta f)\tau_0} e^{-j2\pi \frac{(f_c + \Delta f)}{c_0} \mathbf{U} \cdot \mathbf{a}(\phi, \varphi)}, \quad (1)$$

where  $j = \sqrt{-1}$ ,  $f_c$ ,  $\Delta f$ ,  $\tau_0$ , and  $c_0$  denote the imaginary unit, center frequency, subcarrier spacing, signal delay observed at the center of the UCA, and velocity of light, respectively.  $\zeta := \frac{\lambda}{8R^2} \sqrt{\frac{G_t G_r \sigma_{RCS}}{\pi^3}}$  represents radar channel gain where,  $\lambda = c_0/f_c$ ,  $R = \frac{c_0 \tau_0}{2}$ ,  $G_t$ ,  $G_r$ , and  $\sigma_{RCS}$  denote the wavelength, the target range from the BS, the transmit antenna gain, the receive antenna gain, and the radar cross section, respectively [11]. In this paper, we assume perfect Doppler compensation, and  $\mathbf{U} \in \mathbb{R}^{N \times 3} = [\mathbf{u}_1, \mathbf{u}_2, \dots, \mathbf{u}_N]^T$  represents antenna position matrix where  $\mathbf{u}_n \in \mathbb{R}^3 = [r \cos \frac{2\pi}{N}(n-1), r \sin \frac{2\pi}{N}(n-1), 0]^T$

is a Cartesian coordinate position vector of  $n \in \{1, \dots, N\}$ -th antenna and  $r$  denotes a radius of the UCA. The matrix transpose operation is denoted by  $[\cdot]^T$ , and  $\mathbf{a}(\phi, \varphi) \in \mathbb{R}^3 = -[\cos \phi \cos \varphi, \sin \phi \cos \varphi, \sin \varphi]^T$  is a directional vector where  $\phi \in (0, 2\pi]$  and  $\varphi \in [0, \pi/2]$  denote azimuth and elevation angle, respectively.

In the conventional SPIN-NOMA approach, the ISAC BS transmits sensing signals while receiving communication signals over two time slots. During the second time slot, the ISAC BS transmits a radar signal for target sensing by inverting the phase of the signal transmitted in the first time slot. Thus, the received signal in the  $t \in \{1, 2\}$ -th time slot is given by

$$\mathbf{y}_t = \sum_{k=1}^K \sqrt{\frac{P_k}{2}} \mathbf{h}_k s_{k,t} e^{-j\theta_t} + (-1)^{t-1} \sqrt{\frac{P_R}{2}} \mathbf{g} s_R + \mathbf{w}_t, \quad (2)$$

where  $\sqrt{P_k}$ ,  $\sqrt{P_R}$ ,  $s_{k,t}$ ,  $\theta_t$ ,  $s_R$ , and  $\mathbf{w}_t$  represent the transmit power of the  $k$ -th UE, the power of the sensing signal, the normalized symbol transmitted by the  $k$ -th UE at the  $t$ -th time slot, constellation rotation angle at the  $t$ -th time slot, the normalized sensing signal such that  $\mathbb{E}[|s_{k,t}|^2] = \mathbb{E}[|s_R|^2] = 1$ , and the additive noise vector at the ISAC BS during the  $t$ -th time slot, respectively. All noise components are assumed to be statistically independent and follow a complex Gaussian distribution,  $\mathcal{CN}(\mathbf{0}, \sigma^2 \mathbf{I}_N)$ , where  $\sigma^2$  denotes the noise variance. The term  $(-1)^{t-1}$  indicates the phase inversion applied to the radar signal, where the ISAC BS transmits  $s_R$  in the first time slot and  $-s_R$  in the second time slot. Phase rotation is defined as the operation of rotating the constellation points of a communication signal by a specified angle on the complex plane, implemented by multiplying each symbol with a rotation factor  $e^{-j\theta_t}$ .<sup>1</sup> The value of  $\theta_t$  is predefined and shared between the BS and UEs, allowing the receiver to perform symbol detection based on the rotated constellation. This technique helps prevent symbol ambiguity when different symbols are transmitted across two time slots and superimposed at the receiver [12]. The ISAC BS extracts the communication signal by linearly combining the received signals over the two time slots:

$$\mathbf{y}_{\text{com}} = \frac{\mathbf{y}_1 + \mathbf{y}_2}{\sqrt{2}} = \sum_{t=1}^2 \sum_{k=1}^K \frac{\sqrt{P_k}}{2} \mathbf{h}_k s_{k,t} e^{-j\theta_t} + \frac{\mathbf{w}_1 + \mathbf{w}_2}{\sqrt{2}}. \quad (3)$$

The ISAC BS uses the well-known linear ZF beamformer to detect signals transmitted by multiple UEs with low complexity and low latency as follows [13]:

$$\tilde{\mathbf{y}} \in \mathbb{C}^K = \mathbf{F} \cdot \mathbf{y}_{\text{com}}, \quad (4)$$

where  $\mathbf{F} \in \mathbb{C}^{K \times N}$  represents the pseudo-inverse of the matrix  $\mathbf{H} \in \mathbb{C}^{N \times K} = [\mathbf{h}_1, \mathbf{h}_2, \dots, \mathbf{h}_K]$  as

$$\mathbf{F} = (\mathbf{H}^\dagger \mathbf{H})^{-1} \mathbf{H}^\dagger, \quad (5)$$

where  $\dagger$  denotes a Hermitian operator. Finally, for the signal transmitted by the  $k$ -th UE, the ISAC BS can detect a symbol

<sup>1</sup>The original QPSK constellation in the polar coordinate domain is given by  $\mathcal{S}_{\text{QPSK}} = \{e^{j\frac{\pi}{4}}, e^{j\frac{3\pi}{4}}, e^{j\frac{5\pi}{4}}, e^{j\frac{7\pi}{4}}\}$ . By applying the phase rotation factor, the resulting rotated constellation becomes  $\mathcal{S}_{\text{Rotated}} = \{e^{j(\frac{\pi}{4} - \theta_t)}, e^{j(\frac{3\pi}{4} - \theta_t)}, e^{j(\frac{5\pi}{4} - \theta_t)}, e^{j(\frac{7\pi}{4} - \theta_t)}\}$ .

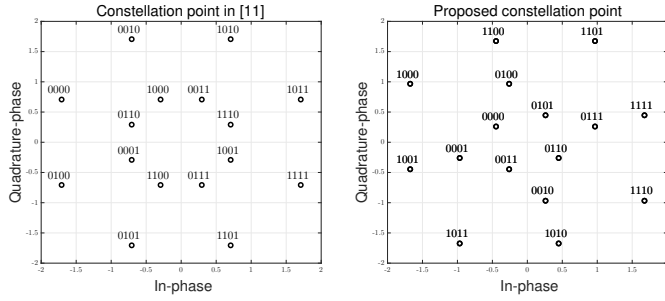


Fig. 2. Proposed constellation design for low-order modulations.

set  $\hat{\mathcal{S}}_k (= \{\hat{s}_{k,1}, \hat{s}_{k,2}\})$  by using the maximum likelihood (ML) detector as

$$\hat{\mathcal{S}}_k = \arg \min_{s_{k,1}, s_{k,2} \in \mathcal{S}_k} \left| \tilde{y}_k - \sum_{t=1}^2 \frac{\sqrt{P_k}}{2} s_{k,t} e^{-j\theta_t} \right|^2, \quad (6)$$

where  $\tilde{y}_k$  represents the  $k$ -th element of  $\tilde{\mathbf{y}}$  vector and  $\mathcal{S}_k$  denotes the candidate set of modulated symbols for  $k$ -th UE.

### III. GENERALIZED SPIN-NOMA FOR ISAC SYSTEMS

#### A. Constellation Design for Low-Order Modulations

In the conventional SPIN-NOMA technique [11], which considered only low-order modulation schemes such as binary phase shift keying (BPSK) and QPSK with *two* communication UEs, phase rotation of communication symbols was introduced over two time slots. Specifically, in [11], to resolve ambiguity between different QPSK signals over two time slots, the phase of one QPSK symbol is rotated, as illustrated on the left side of Fig. 2. However, these existing techniques are not optimized in terms of the minimum distance between constellation points, leaving substantial room for improvement in bit-symbol mapping and phase rotation strategies. In this section, we propose a novel constellation design method that integrates optimized bit-symbol mapping and phase rotation, inspired by [14] and illustrated on the right side of Fig. 2, to maximize the minimum Euclidean distance between adjacent symbols. In the joint constellation points in the form  $s_{k,1}e^{-j\theta_1} + s_{k,2}e^{-j\theta_2}$ , there are two minimum distance candidates,  $\sqrt{4 - 4 \cos \vartheta}$  and  $\sqrt{6 - 4 \cos \vartheta - 4 \sin \vartheta}$ , one is monotonically increasing and the other is monotonically decreasing within the range of 0 to 45 degrees where  $\vartheta := |\theta_1 - \theta_2|$ . Therefore, the minimum distance can be maximized at the point where these two candidates become equal. In this regard, the optimal angle  $\vartheta_{\text{opt}} (= \pi/6)$  is obtained by solving the following equation

$$\sqrt{4 - 4 \cos \vartheta_{\text{opt}}} = \sqrt{6 - 4 \cos \vartheta_{\text{opt}} - 4 \sin \vartheta_{\text{opt}}}. \quad (7)$$

#### B. Novel SPIN-NOMA for High-Order Modulations

The conventional SPIN-NOMA technique lacks scalability for generalized communication systems and makes it difficult to extract sensing signals through a simple linear combination of the received signals over two time slots. To overcome these limitations, we propose an enhanced SPIN-NOMA framework that allows UEs to transmit the same symbol using high-order modulation over two time slots. For instance, instead of the conventional SPIN-NOMA technique, which transmits

different QPSK symbols over two time slots, the proposed framework uses repeated transmission of 16-ary QAM symbols over the same two time slots, achieving the same data rate while improving performance, i.e.,  $s_k := s_{k,1} = s_{k,2}$ . Therefore, the received signal can be expressed as follows:

$$\mathbf{y}_t = \sum_{k=1}^K \sqrt{\frac{P_k}{2}} \mathbf{h}_k s_k + (-1)^{t-1} \sqrt{\frac{P_R}{2}} \mathbf{g} s_R + \mathbf{w}_t. \quad (8)$$

The ISAC BS can then linearly combine the received signals from the two time slots to separately extract the sensing and communication signals as follows.

$$\begin{aligned} \mathbf{y}_{\text{com}} &= \frac{\mathbf{y}_1 + \mathbf{y}_2}{\sqrt{2}} = \sum_{k=1}^K \sqrt{P_k} \mathbf{h}_k s_k + \frac{\mathbf{w}_1 + \mathbf{w}_2}{\sqrt{2}}, \\ \mathbf{y}_{\text{sensing}} &= \frac{\mathbf{y}_1 - \mathbf{y}_2}{\sqrt{2}} = \sqrt{P_R} \mathbf{g} s_R + \frac{\mathbf{w}_1 - \mathbf{w}_2}{\sqrt{2}}. \end{aligned} \quad (9)$$

For the communication function, the ISAC BS performs ML detection for the  $k$ -th UE's signal using the ZF beamformer,  $\tilde{\mathbf{y}} = \mathbf{F} \mathbf{y}_{\text{com}}$ :

$$\hat{s}_k = \arg \min_{s_k \in \mathcal{S}_k} \left| \tilde{y}_k - \sqrt{P_k} s_k \right|^2. \quad (10)$$

#### C. Refined Radar Channel Estimation

In this section, we compare the radar channel estimation accuracy of the conventional SPIN-NOMA scheme with that of the proposed method. The conventional method and the scheme described in Section III-A cannot extract the sensing signal via a linear combination of the received signals. Therefore, the sensing signal must be reconstructed after decoding the communication signals. By applying SIC to remove the communication components from the received signal, the radar signal can be expressed as:

$$\mathbf{y}_{\text{sensing}} = \frac{\mathbf{e}_{\text{SIC}}}{\sqrt{2}} + \sqrt{P_R} \mathbf{g} s_R + \frac{\mathbf{w}_1 - \mathbf{w}_2}{\sqrt{2}}, \quad (11)$$

where  $\mathbf{e}_{\text{SIC}} (\in \mathbb{C}^N)$  is defined as

$$\mathbf{e}_{\text{SIC}} := \sum_{t=1}^2 (-1)^{t-1} \sum_{k=1}^K \sqrt{\frac{P_k}{2}} \mathbf{h}_k (s_{k,t} - \hat{s}_{k,t}) e^{-j\theta_t},$$

which represents the communication signal decoding error. Applying least square estimation (LSE), the radar channel vector is estimated as  $\hat{\mathbf{g}} = \mathbf{y}_{\text{sensing}} / (s_R \sqrt{P_R})$  [11]. Then, the NMSE of the radar channel estimator is given as

$$\begin{aligned} e &= \frac{\mathbb{E}[\|\mathbf{g} - \hat{\mathbf{g}}\|^2]}{\|\mathbf{g}\|^2} = \frac{\mathbb{E}[\|\mathbf{e}_{\text{SIC}} + \mathbf{w}_1 - \mathbf{w}_2\|^2]}{2P_R \|\mathbf{g}\|^2} \\ &= \frac{\mathbb{E}[\|\mathbf{e}_{\text{SIC}}\|^2] + 2\Re\{\mathbb{E}[\mathbf{e}_{\text{SIC}}^\dagger (\mathbf{w}_1 - \mathbf{w}_2)]\}}{2P_R \|\mathbf{g}\|^2} + \frac{N\sigma^2}{P_R \|\mathbf{g}\|^2}, \end{aligned} \quad (12)$$

where  $\Re\{\cdot\}$ ,  $\|\cdot\|$  and  $\mathbb{E}[\cdot]$  denote the real part of the complex number, the Euclidean norm, and the statistical expectation, respectively.

In contrast, the method proposed in Section III-B enables the sensing signal to be separated via a simple linear combination of the received signal, as shown in (9). Applying LSE,

the radar channel vector is obtained by  $\hat{\mathbf{g}} = \mathbf{y}_{\text{sensing}} / (s_R \sqrt{P_R})$ . Then, the NMSE of radar channel estimation is given by:

$$e = \frac{\mathbb{E}[\|\mathbf{g} - \hat{\mathbf{g}}\|^2]}{\|\mathbf{g}\|^2} = \frac{\mathbb{E}[\|\mathbf{w}_1 - \mathbf{w}_2\|^2]}{\|\mathbf{g}\|^2 \cdot 2P_R} = \frac{N\sigma^2}{P_R \|\mathbf{g}\|^2}. \quad (13)$$

It can be seen from (12) and (13) that the proposed technique achieves performance gains by eliminating the impact of communication decoding errors.

#### IV. PERFORMANCE ANALYSIS

We provide a mathematical analysis of the BER performance of the SPIN-NOMA technique based on the signal model described in Section III-B. For simplicity, we begin by analyzing the BER performance and diversity order under the assumption of QPSK modulation. Subsequently, we extend the analysis to a *generalized* QAM signal model.

##### A. Closed-Form BER Analysis for QPSK Modulation

Without loss of generality, we consider only the  $k$ -th UE. After applying the ZF beamformer, the signal corresponding to the  $k$ -th UE can be expressed as follows:

$$\tilde{y}_k = \sqrt{P_k} s_k + \mathbf{f}_{k,:} \cdot \frac{(\mathbf{w}_1 + \mathbf{w}_2)}{\sqrt{2}}, \quad (14)$$

where  $\mathbf{f}_{k,:}$  represents  $k$ -th row of the matrix  $\mathbf{F}$ . Due to the influence of  $\mathbf{f}_{k,:}$ , the noise variance is boosted as follows:  $\mathbb{E}[\|\mathbf{f}_{k,:} \cdot (\mathbf{w}_1 + \mathbf{w}_2) / \sqrt{2}\|^2] = \sigma^2 [(\mathbf{H}^\dagger \mathbf{H})^{-1}]_{k,k}$ , where  $[\cdot]_{a,b}$  represents  $(a, b)$ -th element of the matrix. To achieve this, the noise amplified by the linear ZF beamformer is normalized using a regularization factor, as described in [13], while maintaining the signal-to-noise ratio (SNR).

$$\bar{y}_k = z_k \tilde{y}_k = \sqrt{P_k} z_k s_k + \bar{w}_k, \quad (15)$$

where  $z_k = \sqrt{1/[(\mathbf{H}^\dagger \mathbf{H})^{-1}]_{k,k}}$  denotes regularization factor for  $k$ -th UE.  $\bar{w}_k$  represents the effective noise for  $k$ -th UE, which follows a  $\mathcal{CN}(0, \sigma^2)$  distribution.

From the symmetry of the QPSK constellation, we derive the error probability that the first bit of a symbol  $\{00\}$  is corrupted. For given  $z_k$ , the conditional BER of  $k$ -th UE is given by

$$\Pr(\epsilon_k | z_k) = \Pr(\{00\} \rightarrow \{10\} | z_k) = Q\left(\sqrt{\frac{P_k |z_k|^2}{\sigma^2}}\right), \quad (16)$$

where  $\epsilon_k$  denotes  $k$ -th UE's bit error event and  $Q(\cdot)$  represents  $Q$ -function. Let  $|z_k|^2$  be a random variable  $X_k$ , then the effective channel gain  $X_k$  of  $k$ -th UE statistically follows an Erlang distribution with a shape parameter of  $N - (K - 1)$  and a scale parameter of  $l_k^\alpha$ . Thus, the probability density function of  $X_k$  is as follows:

$$f_{X_k}(x_k) = \frac{l_k^{\alpha(N-K+1)}}{(N-K)!} x_k^{N-K} e^{-l_k^\alpha x_k}. \quad (17)$$

Therefore, from the total probability theorem, the closed form of the  $k$ -th UE's BER can be derived as

$$\Pr(\epsilon_k) = \mathbb{E}_{X_k} \left[ Q\left(\sqrt{\frac{P_k x_k}{\sigma^2}}\right) \right]$$

$$\begin{aligned} &= \int_0^\infty \int_0^\infty \frac{1}{\sqrt{2\pi}} e^{-\frac{\tau^2}{2}} \frac{l_k^{\alpha(N-K+1)} x_k^{N-K}}{(N-K)!} e^{-l_k^\alpha x} d\tau dx \\ &= \frac{1}{2} \left( 1 - \sum_{j=0}^{N-K} \binom{2j}{j} \sqrt{\frac{(P_k/\sigma^2)}{(P_k/\sigma^2) + 2l_k^\alpha}} \cdot \left( \frac{l_k^\alpha}{2(P_k/\sigma^2) + 4l_k^\alpha} \right)^j \right). \end{aligned} \quad (18)$$

##### B. Diversity Order Analysis for QPSK Modulation

In this subsection, we derive the diversity order of the SPIN-NOMA technique, which is defined as

$$\eta_k = - \lim_{\gamma_k \rightarrow \infty} \frac{\log \Pr(\epsilon_k)}{\log \gamma_k}, \quad (19)$$

where  $\gamma_k (= P_k / (l_k^\alpha \sigma^2))$  represents the received SNR about  $k$ -th UE's transmit signal. The diversity order is a widely used metric to characterize the asymptotic behavior of error probability in the high-SNR regime [14]. To determine this, we apply the well-known Taylor series expansion to (18) under the assumption of high transmit SNR. Then, an asymptotic expression can be derived by considering only the first term in the Taylor series expansion as follows

$$\Pr(\epsilon_k) \approx \beta_{N,K} 3^{(N-K+1)} \gamma_k^{-(N-K+1)}, \quad (20)$$

where  $\beta_{N,K}$  denotes the first coefficient in the Taylor series expansion of the BER for  $k$ -th UE and varies according to the number of receive antennas  $N$  and UEs. The value of  $\beta_{N,K}$  can be calculated numerically. Then, the diversity order of the uplink SPIN-NOMA system is given by

$$\eta_k \approx \frac{\log(\beta_{N,K} 3^{N-K+1} \gamma_k^{-(N-K+1)})}{\log \gamma_k} = N - (K - 1). \quad (21)$$

From (21), it is evident that all UEs achieve the same diversity order, regardless of path loss or sensing channel conditions.

##### C. Closed-Form BER Analysis for General M-QAM

In this subsection, we derive a generalized BER expression by leveraging the regular patterns in the bit-error probability. Specifically, an  $M_k$ -ary QAM signal can be regarded as a combination of two independent  $\sqrt{M_k}$ -ary pulse-amplitude modulation (PAM) signals, where  $M_k$  denotes modulation order of  $k$ -th UE. The BER performance of square QAM in additive white Gaussian noise (AWGN) channels is well established [15], and the conditional bit-error probability for the SPIN-NOMA technique in wireless channels can be derived as follows:

$$\Pr(\epsilon_k | z_k) = \frac{1}{\log_2 \sqrt{M_k}} \cdot \frac{2}{\sqrt{M_k}} \sum_{b=1}^{\log_2 \sqrt{M_k}} (1-2^{-b}) \sum_{i=0}^{\sqrt{M_k}-1} \left[ (-1) \left\lfloor \frac{i \cdot 2^{b-1}}{\sqrt{M_k}} \right\rfloor \cdot \left( 2^{b-1} - \left\lfloor \frac{i \cdot 2^{b-1}}{\sqrt{M_k}} + \frac{1}{2} \right\rfloor \right) \right] \cdot Q\left(\frac{(2i+1)d_k}{\sqrt{2}}\right), \quad (22)$$

where  $\lfloor \cdot \rfloor$  denotes the floor function that rounds a given real number down to the nearest integer less than or equal to that number and  $d_k$  represents the minimum distance in signal space expressed as  $d_k = \sqrt{6|z_k|^2 \gamma_k / (M_k - 1)}$ . Then, the

generalized BER performance of the  $k$ -th UE can be derived as

$$\begin{aligned} \Pr(\epsilon_k) &= \mathbb{E}_{X_k} [\Pr(\epsilon_k | z_k)] \\ &= \frac{1}{\log_2 \sqrt{M_k}} \cdot \frac{2}{\sqrt{M_k}} \sum_{b=1}^{\log_2 \sqrt{M_k}} \sum_{i=0}^{(1-2^{-b})\sqrt{M_k}-1} \\ &\left[ (-1)^{\lfloor \frac{i \cdot 2^{b-1}}{\sqrt{M_k}} \rfloor} \cdot \left( 2^{b-1} - \left\lfloor \frac{i \cdot 2^{b-1}}{\sqrt{M_k}} + \frac{1}{2} \right\rfloor \right) \right] \\ &\cdot \left( \frac{1}{2} - \frac{1}{2} \sum_{j=0}^{N-K} \binom{2j}{j} \sqrt{\frac{3(2i+1)^2 \gamma_k}{3(2i+1)^2 \gamma_k + 2(M_k - 1)}} \right. \\ &\cdot \left. \left( \frac{M_k - 1}{6(2i+1)^2 \gamma_k + 4(M_k - 1)} \right)^j \right). \end{aligned} \quad (23)$$

#### D. Diversity Order Analysis for General $M$ -QAM

We derive the diversity order of the uplink SPIN-NOMA technique, assuming  $\sqrt{M_k}$ -ary square QAM signals. An asymptotic expression is derived by considering only the first term in the Taylor series expansion of (23) as

$$\begin{aligned} \Pr(\epsilon_k) &\approx \frac{1}{\log_2 \sqrt{M_k}} \cdot \frac{2}{\sqrt{M_k}} \sum_{b=1}^{\log_2 \sqrt{M_k}} \sum_{i=0}^{(1-2^{-b})\sqrt{M_k}-1} \\ &(-1)^{\lfloor \frac{i \cdot 2^{b-1}}{\sqrt{M_k}} \rfloor} \cdot \left( 2^{b-1} - \left\lfloor \frac{i \cdot 2^{b-1}}{\sqrt{M_k}} + \frac{1}{2} \right\rfloor \right) \\ &\cdot \beta_{N,K} \frac{(M_k - 1)^{(N-K+1)}}{(2i+1)^{2(N-K+1)}} \gamma_k^{-(N-K+1)}. \end{aligned} \quad (24)$$

Then, the diversity order of the uplink SPIN-NOMA system can be derived as  $\eta_k \approx N - (K - 1)$ , which demonstrates that the diversity order of the SPIN-NOMA technique remains unaffected by the modulation order.

### V. SIMULATION RESULTS

In this section, we validate the BER performance of the enhanced SPIN-NOMA system and the mathematical analysis presented in Section IV using Monte Carlo simulations. First, we demonstrate the performance improvements achieved by the proposed rotation angle and bit-to-symbol mapping introduced in Section III. Subsequently, we confirm the accuracy of the performance analysis for the generalized SPIN-NOMA system discussed in Section IV. Fig. 3 illustrates the BER performance of the uplink SPIN-NOMA system under different signal models, based on the received SNR  $\gamma$ . In this simulation, the received SNR ratio between the UEs was set to  $\gamma_1 : \gamma_2 = 4 : 1$  and  $N = 5$ . The results show that the SPIN-NOMA technique outperforms the existing method in [11] when the constellation rotation and bit-to-symbol mapping rules described in Section III-A are applied to the same low-order modulation signal model. Furthermore, the advanced SPIN-NOMA framework in Section III-B, which employs repeated transmission of high-order modulation signals, achieves the best BER performance.

Fig. 4 shows the NMSE of radar channel estimation as a function of the communication SNR for two UEs when  $N = 5$ . We set  $l_1^{-\alpha} = 1$  and  $l_2^{-\alpha} = 4$ . The radar transmit power  $P_R$

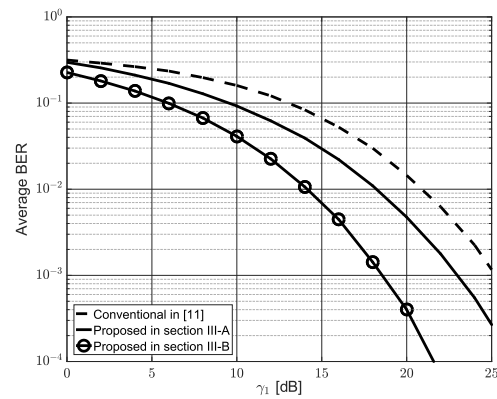


Fig. 3. BER performance of uplink SPIN-NOMA for two UEs when  $\gamma_1 : \gamma_2 = 4 : 1$ ,  $N = 5$ .

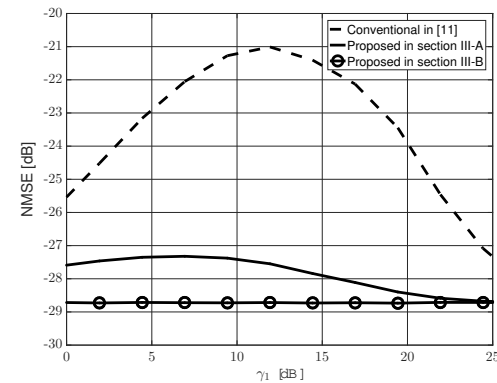


Fig. 4. NMSE of radar channel estimation uplink SPIN-NOMA for two UEs when  $N = 5$ .

is set to 0 dBm, the center frequency  $f_c$  is 5.8 GHz, and the subcarrier spacing  $\Delta f$  is 144 kHz. The noise power spectral density  $N_0$  is set to  $-174$  dBm/Hz, and the noise variance  $\sigma^2$  is computed as  $N_0 \Delta f \approx -123$  dBm. The antenna gains are configured as  $G_t = G_r = 2$ . The radar cross section  $\sigma_{RCS}$  is  $1 \text{ m}^2$ , the radius of UCA  $r$  is 1 m and the target range from the BS  $R$  is 10 m. As shown in (11), both the method in [11] and the scheme described in Section III-A apply SIC to remove the communication signals. In the high-SNR regime, where the BER improves rapidly, the radar channel estimation accuracy increases as the communication SNR increases. However, in the low-SNR regime, where the BER improvement is limited but the communication power continues to increase, the radar channel estimation accuracy tends to degrade with increasing communication SNR. In contrast, the method proposed in Section III-B achieves the best performance and maintains a constant NMSE,  $\frac{N\sigma^2}{P_k \|\mathbf{g}\|^2} \approx -28.72$  dB, regardless of the communication SNR, as derived in (13). This is because the sensing and communication signals are perfectly separated, as shown in (9).

Fig. 5 presents the BER performance of the generalized SPIN-NOMA system described in Section III-B, evaluated for different modulation orders based on the received SNR per bit, i.e.,  $\rho_k = \gamma_k / \log_2(M_k)$ . We consider a scenario with three UEs and five receive antennas at the BS. We also set  $\rho_k$  as  $\rho_1 : \rho_2 : \rho_3 = 4 : 2 : 1$ . For the asymptotic behavior of the BER performance,  $\beta_{N,K}$  is numerically calculated as  $1/6$ ,  $1/12$ , and  $5/108$  for  $N = K$ ,  $N = K + 1$ , and  $N = K + 2$ , respectively.

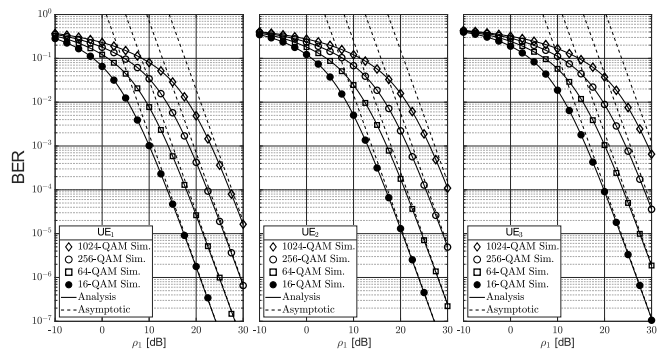


Fig. 5. BER performance of uplink SPIN-NOMA for three UEs when  $\rho_1 : \rho_2 : \rho_3 = 4 : 2 : 1$ ,  $N = 5$ .

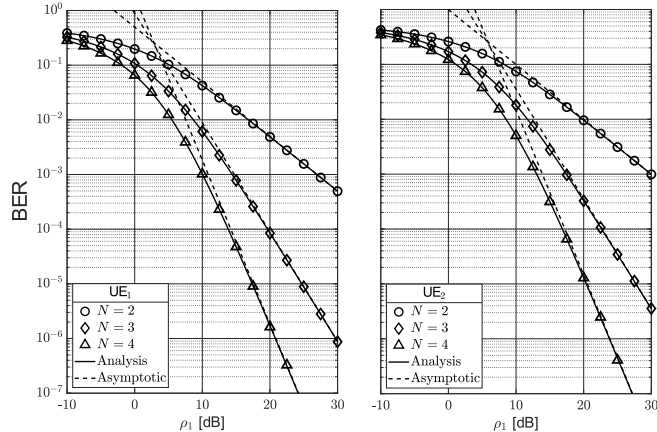


Fig. 6. BER performance of uplink SPIN-NOMA for two UEs considering 16-QAM modulation when  $\rho_1 : \rho_2 = 2 : 1$ .

Fig. 5 confirms that our mathematical analysis aligns closely with the simulation results. In the high-SNR region, the occurrence of bit errors becomes extremely rare, which leads to an increased statistical fluctuation and a corresponding decrease in the reliability of the BER estimates. This is a natural statistical phenomenon and, in fact, further supports that the proposed analytical model accurately approximates the empirical results in a quantitative manner. The BER decreases exponentially in the high-SNR regime, and the slope observed in the log-log scale reflects the system's diversity order. The asymptotic performance in this region aligns almost perfectly with the analytical results, thereby strongly validating the accuracy of the proposed analysis. In particular, identical slopes are observed across different modulation schemes, which confirms that the diversity gain is unaffected by the modulation order, as discussed in Section IV-D.

Fig. 6 illustrates the BER performance of the SPIN-NOMA system with varying numbers of antennas, based on the received SNR per bit. In this simulation, we considered 2 UEs with 16-QAM signals and set  $\rho_k$  as  $\rho_1 : \rho_2 = 2 : 1$ . In Fig. 6, an increase in diversity gain is observed with a higher number of antennas at the BS. As discussed in Sections IV-B and IV-D, the diversity gain is determined solely by the number of UEs and receive antennas. This is clearly confirmed by comparing the case with  $K = 2$ ,  $N = 4$  in Fig. 6 to the case with  $K = 3$ ,  $N = 5$  in Fig. 5. Specifically, when  $K = 2$  and  $N = 4$ , a diversity gain of 3 is achieved, as demonstrated in Section IV-D. This result is consistent with the diversity gain observed in Fig. 5 for  $K = 3$  and  $N = 5$ .

## VI. CONCLUSION

In this paper, we explored an uplink signal phase inversion-based non-orthogonal multiple access (SPIN-NOMA) technique to mitigate mutual interference in next-generation integrated sensing and communication (ISAC) systems. We first identified limitations in the conventional SPIN-NOMA approach and proposed technical enhancements to address these shortcomings. Additionally, we introduced a generalized SPIN-NOMA framework capable of distinguishing communication and sensing signals through a simple linear combination at the base station (BS), while supporting high-order modulation. We then theoretically derived the bit-error rate (BER) performance and diversity order of the generalized SPIN-NOMA technique. Extensive simulations demonstrated that the proposed SPIN-NOMA framework delivers significant performance improvements over the conventional method. Moreover, the theoretical BER analysis closely aligned with the simulation results, further validating the effectiveness of the proposed framework.

## REFERENCES

- [1] N. Wu *et al.*, "AI-enhanced integrated sensing and communications: Advancements, challenges, and prospects," *IEEE Commun. Mag.*, vol. 62, no. 9, pp. 144–150, Sept. 2024.
- [2] N. Wu, H. Li, D. He, A. Nallanathan, and T. Q. S. Quek, "Integrated sensing and communication receiver design for OTFS-based MIMO system: A unified variational inference framework," *IEEE J. Sel. Areas Commun.*, vol. 43, no. 4, pp. 1339–1353, Apr. 2025.
- [3] P. Liu, Z. Fei, X. Wang, Y. Zhou, Y. Zhang, and F. Liu, "Joint Beamforming and offloading design for integrated sensing, communication, and computation system," *IEEE Trans. Veh. Technol.*, Apr. 2025 (early access).
- [4] S. Wang, W. Dai, H. Wang, and G. T. Li, "Robust waveform design for integrated sensing and communication," *IEEE Trans. Signal Process.*, vol. 72, pp. 3122–3138, Jun. 2024.
- [5] Z. Wang, C. Xiao, X. Liu, M. Peng, and J. Guo, "Interference mitigation in multi-cell ISAC systems: A three-dimensional MIMO precoding Approach," *IEEE Wireless Commun. Lett.*, vol. 28, no. 11, pp. 2543–2547, Nov. 2024.
- [6] C. Jia, Z. Zhao, L. Sun, and T. Q. S. Quek, "An interference cancellation scheme of integrated sensing and communications in wireless networks," *IEEE Wireless Commun. Lett.*, vol. 13, no. 12, pp. 3429–3433, Dec. 2024.
- [7] X. Mu, Z. Wang, and Y. Liu, "NOMA for integrating sensing and communications toward 6G: A multiple access perspective," *IEEE Wireless Commun.*, vol. 31, no. 3, pp. 316–323, Jun. 2024.
- [8] C. Ouyang, Y. Liu, and H. Yang, "Revealing the Impact of SIC in NOMA-ISAC," *IEEE Wireless Commun. Lett.*, vol. 11, no. 12, pp. 2685–2689, Dec. 2022.
- [9] L. Sun, Z. Zhao, S. Wang, Z. Ding, and M. Peng, "On the study of non-orthogonal multiple access (NOMA)-assisted integrated sensing and communication (ISAC)," *IEEE Trans. Commun.*, vol. 72, no. 11, pp. 7278–7293, Nov. 2024.
- [10] S. Lv *et al.*, "Short-packet transmission in NOMA-ISAC systems," *IEEE Trans. Cogn. Commun. Netw.*, early access, May 15, 2025, doi: 10.1109/TCCN.2025.3570436.
- [11] H. Liu and E. Alsusa, "A novel ISaC approach for uplink NOMA system," *IEEE Commun. Lett.*, vol. 27, no. 9, pp. 2333–2337, Sept. 2023.
- [12] H. Liu, E. Alsusa, and A. Al Dweik, "Performance analysis of pairwise symbol detection in uplink NOMA-ISaC systems," *IEEE Open J. Commun. Soc.*, vol. 6, pp. 3459–3479, Apr. 2025.
- [13] Y. -S. Lee, K. -H. Lee, H. S. Jang, G. Jo, and B. C. Jung, "Performance analysis of resource hopping-based grant-free multiple access for massive IoT networks," *IEEE Wireless Commun. Lett.*, vol. 11, no. 12, pp. 2685–2689, Dec. 2022.
- [14] K. -H. Lee, J. S. Yeom, J. Jeong, and B. C. Jung, "Performance analysis of uplink NOMA with constellation-rotated STLC for IoT networks," *IEEE Open J. Commun. Soc.*, vol. 3, pp. 705–717, Apr. 2022.
- [15] K. Cho and D. Yoon, "On the general BER expression of one- and two-dimensional amplitude modulations," *IEEE Trans. Commun.*, vol. 50, no. 7, pp. 1074–1080, Jul. 2002.